

Light Curve Calculations of Supernovae from Fallback Gamma-Ray Bursts

Chris L. Fryer^{1,2}, Aimee L. Hungerford¹, Patrick A. Young^{3,4}

fryer@lanl.gov, aimee@lanl.gov, payoung@lanl.gov

ABSTRACT

The currently-favored model for long-duration gamma-ray bursts (GRBs) invokes explosions from the collapse of a massive star down to a black hole: either directly or through fallback. Those GRBs forming via fallback will produce much less radioactive nickel, and hence it has been argued (without any real calculation) that these systems produce dim supernovae. These fallback black-hole GRBs have been recently been argued as possible progenitors of a newly discovered set of GRBs lacking any associated supernovae. Here we present the first ever radiation-hydrodynamics calculations of the light-curves produced in the hypernova explosion by a delayed-fallback gamma-ray burst. We find that the bolometric light-curve is dominated by shock-deposited energy, not the decay of radioactive elements. As such, observations of such bursts actually probe the density in the progenitor wind more than it does the production of radioactive nickel.

Subject headings: Gamma Rays: Bursts, Nucleosynthesis, Stars: Supernovae: General

1. Introduction

It is now generally accepted that long-duration GRBs are associated with bright supernova-like explosions. One of the primary differences between these GRB-associated “supernovae” and normal supernovae is that GRB-associated supernovae have larger (by more than a

¹Computational Methods, Los Alamos National Laboratories, Los Alamos, NM 87545

²Physics Dept., University of Arizona, Tucson AZ 85721

³Applied Physics, Los Alamos National Laboratories, Los Alamos, NM 87545

⁴Steward Observatory, University of Arizona, Tucson AZ 85721

factor of 4 in some cases) ^{56}Ni yields. How is this extra ^{56}Ni produced. It is known that the GRB jets themselves do not produce large amounts of ^{56}Ni and researchers focused on two different paradigms for producing large amounts of ^{56}Ni : the ^{56}Ni is produced in a disk around the black hole (see Surman et al. 2006 and references therein), or the ^{56}Ni is produced in the explosion of the star that accompanies the GRB jet (e.g. Nagataki et al. 2003; Mazzali et al. 2006). Calculations assuming an accretion-disk site for ^{56}Ni production tend to approximate the disk using the structure from advection dominated accretion flow solutions (e.g. Popham et al. 1999) and use a neutrino-driven wind solution to derive particle trajectories. Depending upon the exact conditions in the disk (in particular, the electron fraction), a large amount of ^{56}Ni can be produced. Although Surman et al. (2006) have shown that the amount of ^{56}Ni produced does depend upon the conditions in the disk, one can reasonably assume that this mechanism always produces large amounts of ^{56}Ni .

The explosive nucleosynthesis site uses strong shocks in the stellar explosion (beyond the narrow jet region) to heat material and cause it to burn to ^{56}Ni . It depends sensitively on the structure of the star and the velocity of the shock beyond the jet itself. Nomoto and collaborators (Maeda & Nomoto 2003; Nomoto et al. 2004) have argued that a significant portion of the star in a GRB is still ejected in faster-than-normal velocities, allowing the production of enhanced amounts of ^{56}Ni . The problem with this site of ^{56}Ni production is that GRBs may be produced both as direct collapse black holes or through weak supernovae that do not impart enough energy onto the star to prevent the fallback of matter onto the proto-neutron star, causing it to collapse to a black hole. Fryer et al. (2006) found that if the delay between this weak supernova explosion is more than a few seconds, the amount of ^{56}Ni produced in explosive nucleosynthesis is very small indeed. And with very little ^{56}Ni produced in the explosion, these GRBs should produce dim supernovae.

Where are these GRBs with faint associated supernovae? All observations suggested that bursts were associated with bright, high ^{56}Ni -yield, high-velocity supernovae (also known as “hypernovae” - Nomoto et al. 2004). Could it be that fallback black holes do not produce GRBs? The same month the Fryer et al. (2006) paper was accepted, the first of two very peculiar long-duration bursts exploded. These two bursts were well-localized, but their late-time emission showed no presence of an associated supernova (Fynbo et al. 2006, Gal-Yam et al. 2006). On the surface, these bursts seem to be exactly the dim-Supernova GRBs predicted by theory. But Gal-Yam et al. (2006) argue that GRB060614 is not a typical long burst and may require a different engine altogether. GRB060605’s duration ($T_{90} = 4 \pm 1$ s) lies on the border between short and long bursts and Ofek et al. (2007) argue that it is a short burst. So the observational evidence of low ^{56}Ni -yield GRB-supernovae is far from conclusive.

In addition, we must be wary of making any strong claims between ^{56}Ni yields and supernova light-curves. The process by which the energy from the decay of ^{56}Ni and its daughter product ^{56}Co is converted into optical photons is not linear. The energy from decay is released in gamma-rays which then scatter and ultimately absorb in the star. The star thermalizes this energy and re-emits it in optical photons. But the star is also hot because it just exploded and the shock energy has heated it. In supernovae, the peak of the supernova light-curve can be powered either by this shock energy or, for the most compact stars, the decay of radioactive material. In this paper, we provide the first radiation-hydrodynamics explosion calculations of these delayed-collapse hypernovae. In §2, we describe both our initial stellar models and a description of our light-curve code. We conclude with a discussion of our results and comparison of these results to the current data.

2. Initial Conditions and Code Description

For initial conditions, we use the two 40 M_{\odot} fallback GRBs from (Fryer et al. 2006a) with two different delays between the weak supernova explosion and the GRB outburst: a 1 s delay producing 0.33 M_{\odot} of ^{56}Ni , and a 6.8 s delay producing 0.016 M_{\odot} . We will focus on the longer delay explosion in our efforts to produce a dim supernova explosion. At early times, the radiation is completely trapped, so we grab the models from these calculations after the shock has moved a few times 10^9 cm . Fryer et al. (2006a) calculated the detailed yields from these models, but for our opacities we have reduced these yields to 30 base elements from hydrogen up to zinc. Figure 1 shows the initial velocity structure used in our models. Note that these explosions are very fast with shock velocities v_{shock} in excess of $2 \times 10^9\text{ cm s}^{-1}$, and the stars are rather compact ($1.5 \times 10^{10}\text{ cm}$) so the shock will quickly break out of the star.

On top of this basic stellar structure, we have added a wind structure using the mass loss rates from the last $\sim 10,000\text{--}100,000\text{ y}$ in the life of our Wolf-Rayet stars based on models presented by Fryer et al. (2006b): $2 \times 10^{-5}\text{ M}_{\odot}\text{ y}^{-1}$ with velocities in the 700 km s^{-1} range. Note that the wind velocities could be as high as $3,000\text{ km s}^{-1}$ and it is likely that GRBs arise from lower metallicity objects where the mass-loss rate is lower than our chosen values. The primary effect of both of these is a lowering of the density in the wind. We have included a run where the density is scaled down by a factor of 100 to study this effect. The initial density profile of all our models are shown in fig. 1.

For our calculations, we use the multidimensional radiation-hydrodynamics code RAGE (Radiation Adaptive Grid Eulerian), which was designed to model a variety of multimaterial flows (Baltrusaitis et al. 1996). The conservative equations for mass, momentum, and total energy are solved through a second-order, direct-Eulerian Godunov method on a finite-

volume mesh (Gittings et al. 2007). It includes a flux-limited diffusion scheme to model the transport of photons using the Levermore-Pomraning flux limiter (Levermore & Pomraning 1991). RAGE has been extensively tested on a range of verification problems (Holmes et al. 1999; Hueckstaedt et al. 2005) and applied to (and tested on) a range of astrophysics problems (Herwig et al. 2006; Coker et al. 2006; Fryer et al. 2007), including the strong velocity gradients that exist in supernova explosions (Lowrie & Rauenzahn 2006).

The RAGE code can be used in 1, 2, and 3 dimensions with spherical, cylindrical and planar geometries in 1-dimension, cylindrical and planar geometries in 2-dimensions, and planar geometries in 3-dimensions. For this paper, we focus on 1-dimensional, spherical calculations. RAGE uses an adaptive mesh refinement technique, allowing us to focus the resolution on the shock and follow the shock as it progresses through the star. Even so, we were forced to regrid in our calculations to ensure that we resolved the shock at early times but still allow us to model the shock progression out to 100 d (the shock moves from 10^9 cm out to 10^{16} cm in the course of a simulation).

For our current set of calculations, the energy released from the decay ^{56}Ni and ^{56}Co is deposited directly at the location of the ^{56}Ni using the following formula:

$$dE/dt = E_{\text{Ni}}/\tau_{\text{Ni}}e^{-t/\tau_{\text{Ni}}} + E_{\text{Co}}/(\tau_{\text{Co}} - \tau_{\text{Ni}})[e^{-t/\tau_{\text{Co}}} - e^{-t/\tau_{\text{Ni}}}] \quad (1)$$

where $E_{\text{Ni}} = 1.7 \text{ MeV}$ and $E_{\text{Co}} = 2.9 \text{ MeV}$ are the mean energies released per atom for the decay of ^{56}Ni and ^{56}Co , respectively, and $\tau_{\text{Ni}} = 7.6 \times 10^5 \text{ s}$, $\tau_{\text{Co}} = 9.6 \times 10^6 \text{ s}$. Especially at late times, this energy is not deposited into the matter surrounding it, but rather escapes the star. We have included a simulation where after the shock has reached $5 \times 10^{12} \text{ cm}$, we assume 99% of the energy escapes, allowing a lower bound on our models. This provides us with 4 models in total: 1 s delay, 6.8 s delay, 6.8 s delay with large escape fraction of gamma-rays, and a 6.8 s delay with both a large escape fraction and a lowered wind.

For opacities, we use the SESAME opacities produced at LANL (Magee et al. 1995). These opacities have been extensively used in astrophysics including many problems in supernovae (e.g. Fryer et al. 2000; Deng et al. 2005; Mazzali et al. 2006). This opacity base is being continually updated, and we use the latest updates on these opacities. The assumption with these opacities is that the atoms are in local thermodynamic equilibrium with the matter and, hence, the opacity can be determined assuming a single temperature in each cell. Only a few atoms deviate significantly from their local thermodynamic solution and this affect should be minor for our calculations of bolometric light curves.

3. Theoretical Light Curves and the Observations

If there still is considerable internal energy in the shock when it reaches the edge of the star, the shock can accelerate even further when it reaches the wind. From figure 1, we see this is the case for our short delay model, but not for our long delay models. At this time, roughly 4×10^4 s (3×10^4 s for our short delay model) the shock is just becoming optically thin. This occurs between $5 - 10 \times 10^{13}$ cm when the shock is well beyond the stellar surface and out in the Wolf-Rayet wind. For our short-delay model, the shock has taken on a homologous velocity ($v \propto r$) structure, but the long-delay models take more than 10^5 s to develop the canonical homologous velocity structure. More important, note the density structure in these models. In the long-delay models, the weak supernova shock combined with the accretion of fallback material produces an evacuated region around the compact remnant. When the strong explosions sweeps up the weak supernova shock, it produces a shell of fast moving material. This ring of material causes the shock to remain optically thick longer than one would expect from more standard shock profiles¹. Clearly, the nature of the explosion will have a strong affect on our light-curves. Simple, homologous-velocity profiles, with power-law density profiles will not be able to model the broad range of explosion scenarios.

The short-delay explosion experiences both a shock break-out bump at 3 days followed by a ^{56}Ni -powered peak at roughly 25 days after the launch of the explosion. The only surprise in this model is that shock break-out for these strong explosions propagating through dense wind material can produce strong emission, in excess of $10^{44} \text{ ergs s}^{-1}$! This emission becomes the dominant emission in models where the ^{56}Ni is small. The light-curves produced by our long-delay (\equiv low ^{56}Ni yield) simulations are shown in figure 2. These light-curves only get a large peak at shock break-out. This sharp peak drops within 8 days of the launch of the explosion. By allowing the gamma-rays to escape, we actually get a brighter peak luminosity (the shock is slightly more compact and is hotter), but by 20 days, the model with 100% gamma-ray deposition is brighter and by 100 d it has a luminosity that is an order of magnitude higher than the model with only 1% gamma-ray deposition.

These features can be explained if the bulk of the light-curve is powered by shock energy, not gamma-ray deposition. The peak in the light curve is powered by shock break-out. Indeed, it appears that shock energy dominates out beyond 20-30 days. The fact that the supernova explosion is strong ($\gtrsim 10^{52}$ erg) and the ^{56}Ni production is low ($< 0.02 M_{\odot}$), this is not unexpected. In such a system, one would expect that the amount of mass in the

¹Note that at these early times, the short-delay models with and without the loss of ^{56}Ni decay gamma-rays are identical.

wind is more important. Our simulation with a low wind is an order of magnitude dimmer than our strong wind candidates.

The strong shock drives the matter temperature (and the emitted Planck-averaged radiation temperature) well beyond the optical bands. But as the shock moves out of the envelope, the averaged radiation energy in the shock decreases (Fig. 3). It is the temperature in the shocks that drive most of the emission and this temperature is characteristic of the radiation temperature. 6 days into the explosion, when the luminosity peaks, the Planck-averaged radiation temperature lies between 1.5-4eV for all models, with most of the photons emerging in the ultraviolet.

Let's compare these models with the observational limits placed by Fynbo et al.(2006) and Gal-Yam et al. (2006). At 10 days for a GRB at 388 Mpc (roughly equivalent to a redshift of 0.089 corresponding to GRB060505), the bolometric luminosities for these three models are 23.5, 24.7, and 26.8 magnitudes for the 1% gamma-ray deposition, 100% gamma-ray deposition, and low wind models respectively. For the more distant GRB060614, the expected late-time flux is even lower. It is likely that these models would all be below the observed limits at this time.

However, at shock break-out, these spherically-symmetric models predict a very bright luminosity (above 20th magnitude at 6 d). Why don't we see the burst at this time? Although the afterglow is still strong at this time, our predicted luminosities could well dominate. But remember that the peak flux is in the ultraviolet, not the optical. The fact that nothing is observed could place constraints on the model. Either there is considerable dust extinction (a few magnitudes in the UV), the explosion is weaker than our spherically symmetric 10^{52} erg explosion has assumed, or this GRB truly is different than our standard long-duration burst classification as Gehrels et al. (2006) and Gal-Yam et al. (2006) argue.

We have learned a number of features of delayed black-hole forming GRBs. First, the emission of these supernovae are likely to peak at shock break-out. The luminosity is dominated by the shock energy, and not the decay of radioactive elements. As such, any observation places more constraints on the surrounding wind than it does on the ^{56}Ni yield. Also, the structure of the shock may well be very different than the canonical density and velocity structures seen in more normal supernovae and we must pay particular attention to the explosions in calculating these light-curves. The models in these papers are examples of a larger set of possibilities. Finally, bear in mind that we are assuming spherically symmetric models run in the gray approximation and asymmetric, multi-group models may have very different light-curves.

This work was carried out in part under the auspices of the National Nuclear Security

Administration of the U.S. Department of Energy at Los Alamos National Laboratory and supported by Contract No. DE-AC52-06NA25396.

REFERENCES

- Baltrusaitis, R., Gittings, M., Weaver, R., Benjamin, R., & Budzinski, J. 1996, *Phys. Fluids*, 8, 2471
- Coker, R.,F. et al. 2006, *Ap&SS*, 579
- Deng, J., Tominaga, N., Mazzali, P.A., & Maeda, K. 2005, *ApJ*, 624, 898
- Fryer, C.L., Colgate, S.A., Pinto, P.A. 1999, *ApJ*, 511, 885
- Fryer, C.L., Rockefeller, G., & Young, P.A. 2006, *ApJ*, 647, 1269
- Fryer, C.L., Young, P.A., & Hungerford, A.L. 2006, *ApJ*, 650, 1028
- Fryer, C.L., Hungerford, A.L., & Rockefeller, G. 2007, submitted to the *International Journal of Modern Physics D*.
- Fynbo, J.P.U. et al. 2006, *Nature*, 444, 1047
- Gal-Yam et al. 2006, *Nature*, 444, 1053
- Gehrels, N., et al. 2006, *Nature*, 444, 1044
- Gittings, M., et al. 2006, *J. Comput. Phys.*, submitted
- Herwig, F., Freytag, B., Hueckstaedt, R.M., Timmes, F.X. 2006, *ApJ*, 642, 1057
- Holmes, R. et al. 1999, *J. Fluid Mech.*, 389, 255
- Hueckstaedt, R., et al. 2005, *Ap&SS*, 298, 255
- Levermore, C.D., & Pomraning, G.C. 1981, *ApJ*, 248, 321
- Lowrie, R.B., & Rauenzahn, R.M. 2006, LANL Technical Reports, LA-UR-06-3853
- Maeda, K. & Nomoto, K. 2003, *ApJ*, 598, 1163
- Magee, N.H., Jr., Abdallah, J., Jr., Clark, R.E.H. et al. *PASP Conference Series, Astrophysical Applications of Powerful New Databases*, eds. S. J. Adelman and W.L. Wiese, 78, 51

Mazzali, P.A. et al. 2006, ApJ, 645, 1323

Nagataki, S., Mizuta, A., Yamada, S., Takabe, H., & Sato, K. 2003, ApJ, 596, 401

Nomoto, K., Maeda, K., Mazzali, P.A., Umeda, H., Deng, J., & Iwamoto, K., in “Stellar Collapse”, Astroph. & Space Science Library, ed. Chris Fryer, Kluwer Academic Publishers (Dordrecht)

Ofek et al., in preparation

Popham, R., Woosley, S.E., & Fryer, C. 1999, ApJ, 518, 356

Surman, R., McLaughlin, G.C., & Hix, W.R. 2006, ApJ, 643, 1057

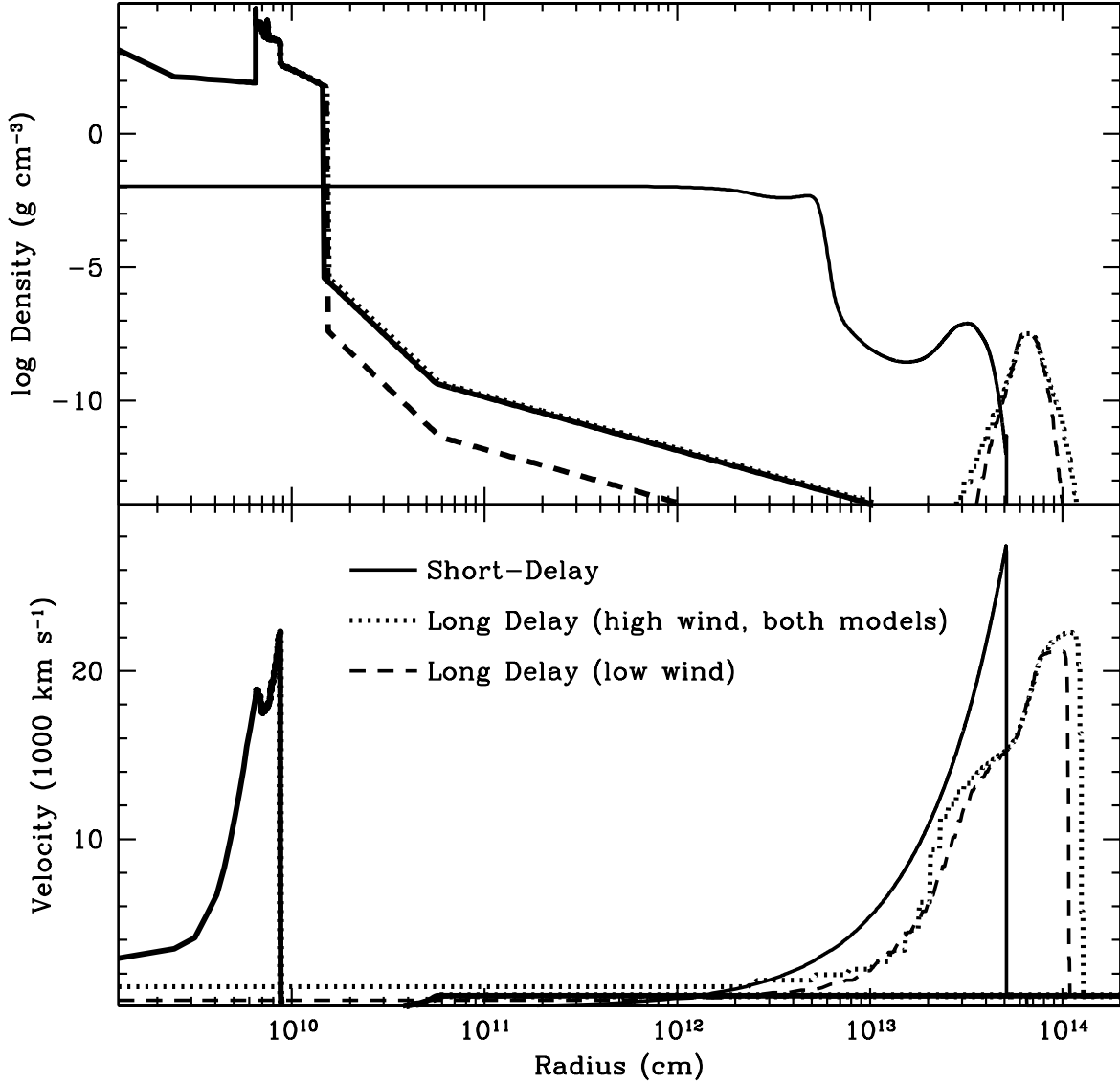


Fig. 1.— Density versus radius (top) of our explosion models when we map the model into RAGE and after $4 \times 10^4 \text{ s}$ ($3 \times 10^4 \text{ s}$ for our short delay model). The solid line corresponds to our short-delay model, the dotted line to our long-delay models (the model with full energy deposition and the model assuming 99% of the energy escapes look very similar at this point), and the dashed line corresponds to our long delay model with the lowered winds. Note that density has a peak near the shock. This is because most of the matter is moving at the same, very-high velocity. The bottom panel shows the velocity versus radius for these same models. The short-delay model has accelerated as it expands. At these early times the long-delay models have not yet developed into a homologous outflow.

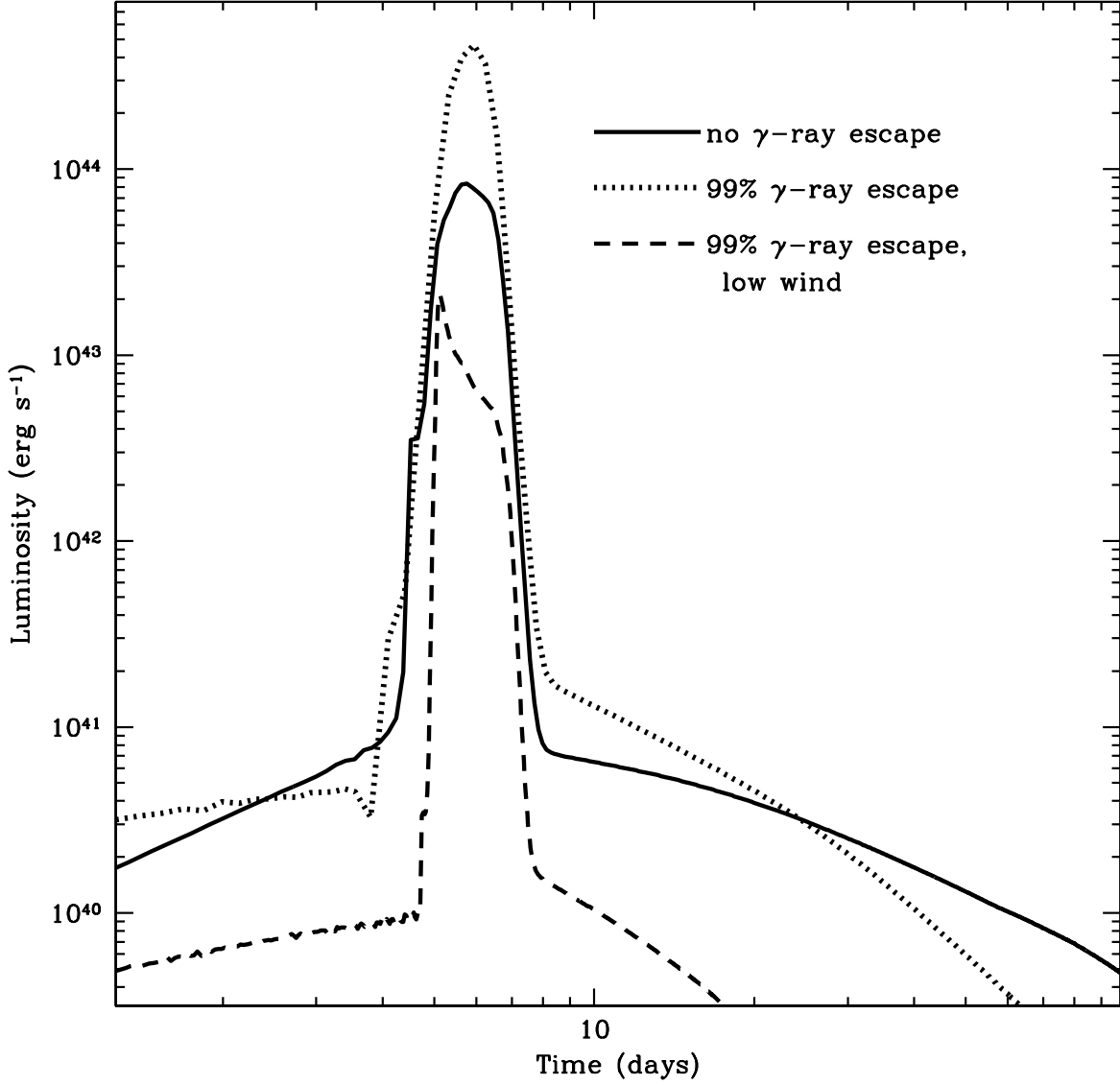


Fig. 2.— Luminosity versus time for our 3 long-delay simulations: full energy deposition (solid), 99% energy loss (dotted), and the low-wind model with 99% energy loss (dashed). The peak in the light-curve is powered by shock breakout. It happens early (6 days) and decays considerably by 8 days. By 10 days, the bolometric luminosity for the low wind model is below 10^{40}ergss^{-1} . The peak in the light curve is not sensitive to the ^{56}Ni yield, but to the energy of the explosion and the mass in the wind.

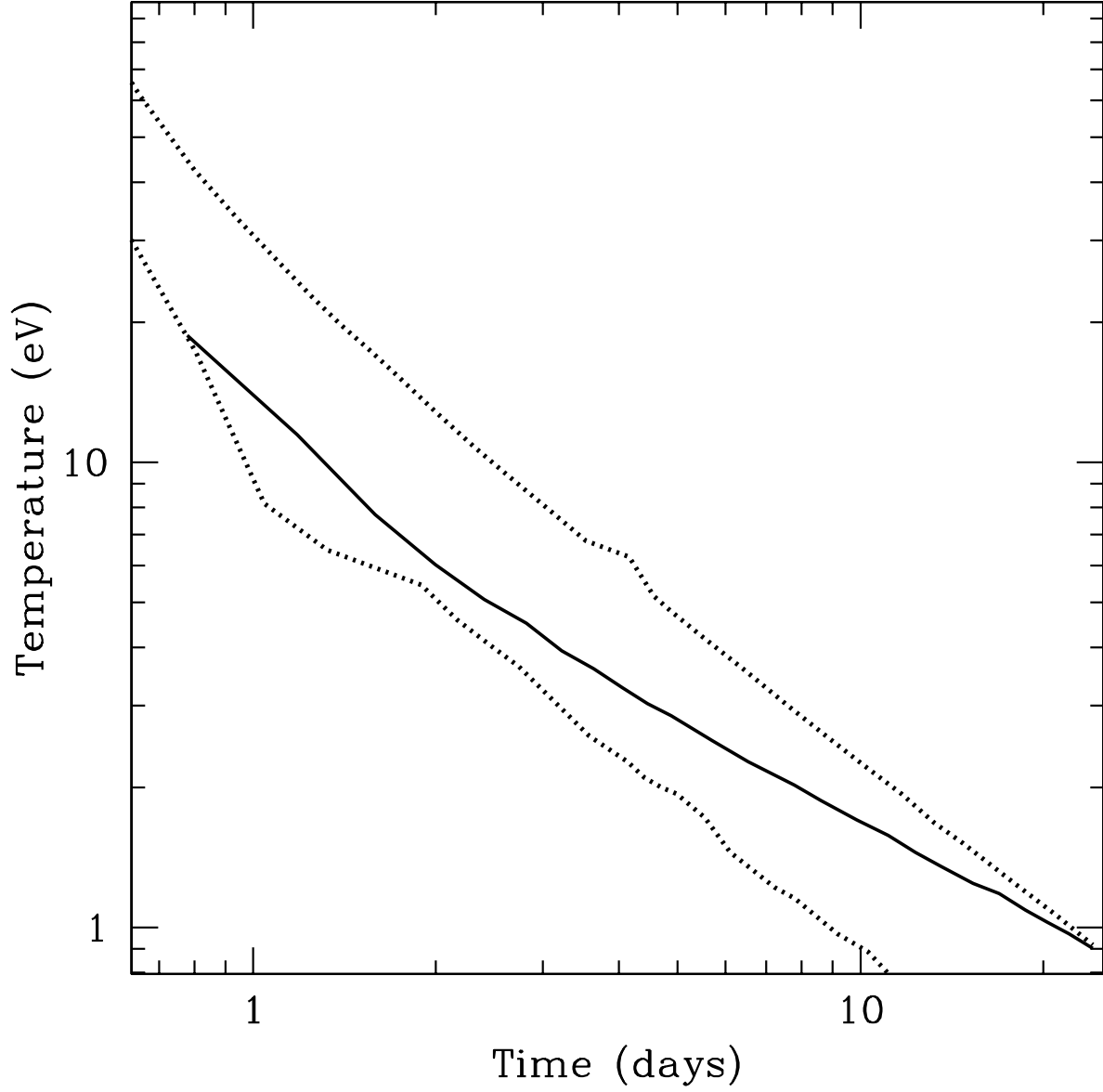


Fig. 3.— Planck-averaged temperature of the radiation in the shock as a function of time. Recall that the peak in the emission occurs at a wavelength at $\lambda_{\text{peak}} \approx 250/T_{\text{eV}}\text{nm}$ where T_{eV} is the temperature in eV. The peak in the luminosity occurs at roughly 6 days for all of our models, and the bulk of the emission is radiated in the ultraviolet.